
Nanoplastics exposure modulate lipid and pigment compositions in diatoms

Gonzalez-Fernandez Carmen ^{1,4}, Le Grand Fabienne ², Bideau Antoine ⁴, Huvet Arnaud ³, Paul-Pont Ika ², Soudant Philippe ^{2,*}

¹ Fish Innate Immune System Group, Department of Cell Biology and Histology, Faculty of Biology, Regional Campus of International Excellence "Campus Mare Nostrum", University of Murcia, 30100, Murcia, Spain

² Laboratoire des Sciences de l'Environnement Marin (LEMAR), Univ. Brest, CNRS, IRD, Ifremer, LEMAR, F-29280, Plouzané, France

³ Ifremer, Laboratoire des Sciences de l'Environnement Marin (LEMAR), CS 10070, 29280, Plouzané, France

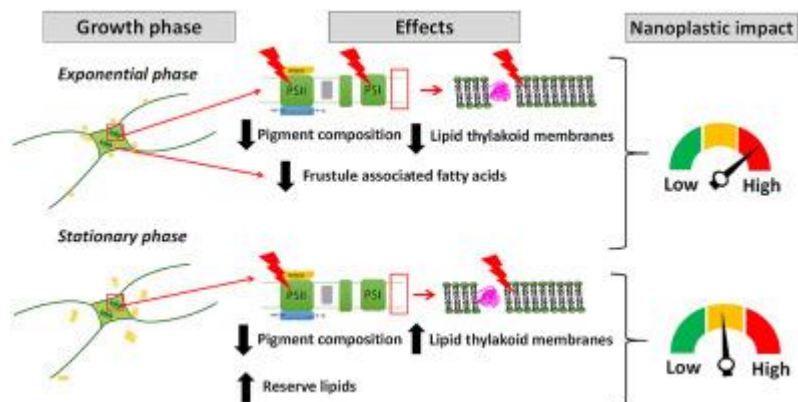
⁴ Laboratoire des Sciences de l'Environnement Marin (LEMAR), Univ. Brest, CNRS, IRD, Ifremer, LEMAR, F-29280, Plouzané, France

* Corresponding author : Philippe Soudant, email address : philippe.soudant@univ-brest.fr

Abstract :

The impact of nanoplastics (NP) using model polystyrene nanoparticles amine functionalized (PS-NH₂) has been investigated on pigment and lipid compositions of the marine diatom *Chaetoceros neogracile*, at two growth phases using a low (0.05 µg mL⁻¹) and a high (5 µg mL⁻¹) concentrations for 96 h. Results evidenced an impact on pigment composition associated to the light-harvesting function and photoprotection mainly at exponential phase. NP also impacted lipid composition of diatoms with a re-adjustment of lipid classes and fatty acids noteworthy. Main changes upon NP exposure were observed in galactolipids and triacylglycerol's at both growth phases affecting the thylakoids membrane structure and cellular energy reserve of diatoms. Particularly, exponential cultures exposed to high NP concentration showed an impairment of long chain fatty acids synthesis. Changes in pigment and lipid content of diatom' cells revealed that algae physiology is determinant in the way cells adjust their thylakoid membrane composition to cope with NP contamination stress. Compositions of reserve and membrane lipids are proposed as sensitive markers to assess the impact of NP exposure, including at potential predicted environmental doses, on marine organisms.

Graphical abstract



Highlights

► Nanoplastics (NP) effect on algae was studied at exponential and stationary phase. ► NP impact pigment and lipid composition of diatoms at both growth phases. ► Algae adjust their thylakoid membrane lipid composition to cope with NP stress. ► Algae physiological state is a determinant factor to evaluate NP impact on diatoms.

Keywords : diatoms, nanoplastics, lipid composition, pigments

38 **Introduction**

39 Plastics, with their many useful physical and chemical properties, are widely used in
40 various industries and activities of daily living. With an increasing year production,
41 plastics exceed 300 million tons annually (Plastics Europe, 2016). Polystyrene (PS) is
42 one of the most largely used plastics worldwide, in food and industry packaging,
43 disposable cutlery, medical products and toys, between other applications (Plastics
44 Europe, 2016). Plastic materials pose a serious threat to the marine environment when
45 not properly disposed or recycled. Approximately the 10% of the annual plastic
46 production ends up into the oceans (Avio et al., 2015). Once in the environment, plastic
47 debris fragments into smaller particles such as microplastics (MP; < 5 mm) and
48 presumably nanoplastics (NP; < 100 nm; Amaral-Zettler et al., 2016). Because of its
49 fundamental role in marine ecosystem's net primary productivity, an increasing number
50 of studies have paid attention to the ecological impact of MP in phytoplankton
51 (Bhattacharya et al., 2010; Lagarde et al., 2016; Long et al., 2017, 2015; Sjollem et al.,
52 2016; Zhang et al., 2017). Nevertheless, when particle size reached millimeter-scale,
53 MP had fewer impacts on growth of marine microalgae (Zhang et al., 2017). Stronger
54 effects were observed when plastic particle size decreased down to nano-size
55 (González-Fernández et al., 2019; Manfra et al., 2017; Mao et al., 2018; Nolte et al.,
56 2017). Furthermore, the small size of NP can favor their pass through the lipid bilayer
57 of biological membranes and affect the functioning of cells, including lipid metabolism
58 (Bergmann et al., 2015). Indeed, due to nano-properties (nano-size, high surface-to-
59 volume ratio), NP can induce high toxicity notably on early life stages (e.g. Balbi et al.,
60 2017; Della Torre et al., 2014; Pinsino et al., 2017 ; Tallec et al., 2018).

61 Diatoms are unicellular, mainly photosynthetic, eukaryotes living within elaborate
62 silicified cell walls and claimed to be responsible for around 40% of global primary

63 productivity in the oceans (Prihoda et al., 2012). Lipids are the major constituents of
64 diatom cells and the average lipid content in diatoms could account up to 25% of dry
65 weight (Levitan et al., 2014), although the production of lipids in diatoms can vary
66 according to culture conditions (Yi et al., 2017). Among the lipids produced by diatoms,
67 polyunsaturated fatty acids (PUFA) such as eicosapentaenoic acid (EPA, 20:5n-3), are
68 essential in the nutrition of benthic and pelagic animals. Feeding on phytoplankton,
69 marine arthropods and vertebrates incorporate diatom PUFA into their own lipid
70 composition, and thus become an important source of these lipids in human nutrition
71 (Dolch and Marechal, 2015).

72 It is generally accepted that the ability of algae to adapt to environmental conditions is
73 reflected in a great variety of lipid patterns as well as with their ability to synthesize a
74 number of unusual lipidic compounds (Guschina and Harwood, 2006). These
75 fluctuations in microalgae lipid composition and the resulting change in their membrane
76 physical properties can have significant influence on their physiology and later affecting
77 higher trophic levels. Considering the importance of lipid production by diatoms and
78 their relevance in trophic energy transfer and ecosystem functioning, the aim of this
79 work was to identify the impact of small NP (50 nm PS-NH₂) on lipid metabolism and
80 composition of microalgae at two growth phases. The presence of NH₂ groups on
81 micro- and nanoplastics in natural environments seems unlikely as plastic debris tends
82 to have more carboxylated surfaces than anionic surfaces due to the oxidation processes
83 following UV radiations (Fotopoulou and Karapanagioti, 2012; Ter Halle et al., 2016).
84 Nevertheless PS-NH₂ constitutes excellent model particles to study the interactions
85 between nanoplastics and live cells as they remain stable in seawater and their cationic
86 surfaces promotes interactions with negatively charged biological membranes (Tallec et
87 al., 2019).

88 According to model predictions, by the 2060s, concentrations of MP will reach around 1
89 $\mu\text{g mL}^{-1}$ for MP higher than 0.3 millimeters (Isobe et al., 1957; Lenz et al., 2015).
90 Although the real concentrations of small NP in the marine environment is unknown,
91 for NP around 50 nm it has been predicted to be environmentally relevant
92 concentrations below $0.015 \mu\text{g mL}^{-1}$ (Al-sid-cheikh et al., 2018). In our study, *C.*
93 *neogracile* cultures at exponential and stationary growth phases were exposed for 96
94 hours to two NP concentrations 0.05 and $5 \mu\text{g mL}^{-1}$. The effects of NP were evaluated
95 on membrane and reserve lipids (lipid class and fatty acid composition).

96 Biosynthesis and homeostasis of lipids strongly affect chloroplast development
97 (Kobayashi, 2018) potentially impacting the photosynthetic machinery. The function of
98 the photosynthetic process in diatoms is the capture of light energy by pigments
99 (Lavaud, 2007). Most of them are localized in the thylakoid membranes (Kuczynska et
100 al., 2015). Taking into account the importance that lipid have on formation of
101 membrane structures and photosensitive pigments, the pigment composition of *C.*
102 *neogracile* upon exposure to NP was also investigated.

103 In the context of NP pollution, the presence of colloids and natural organic matter in the
104 media can affect NP behavior and potential toxicity (Manfra et al., 2017; Galloway et
105 al., 2017). Particularly diatoms are recognized for producing exopolysaccharides (EPS)
106 that may rearrange to form larger particles, the transparent exopolymeric particles (TEP;
107 Mari et al., 2017). NP behaviour in exponential and stationary cultures as well as its
108 impact on cellular and metabolic responses of *C. neogracile* cells were studied in
109 González-Fernández et al. (2019). The present study take part of the same experiment
110 and aims to go further evaluating the effect of 50 nm PS-NH₂ on lipid and pigment
111 compositions of diatom cells.

112 2. Material and methods

113 2.1. Microalgae culture and exposure

114 Batch cultures of *Chaetoceros neogracile* (strain CCAP 1010-3), were grown in 500 mL
115 balloons (24 h light cycle, 100 $\mu\text{moles photons m}^{-2} \text{ s}^{-1}$ at 20 °C) in constant aeration
116 within CO₂ supplementation. For cultures inoculation, two sets of cultures were
117 prepared with a 7 days interval in order to expose them in exponential growth phase and
118 in stationary growth phase to NP (González-Fernández et al., 2019).

119 For exposure, concentrations of both batch cultures were adjusted at 4×10^5 cells mL⁻¹
120 by centrifugation (550 g during 5 minutes) and resuspension of cells in a final volume
121 of 300 mL of their corresponding media (exponential vs. stationary media). Cultures
122 were exposed to fluorescent-blue 50 nm amino (PS-NH₂) polystyrene nanoparticles
123 purchased from Sigma-Aldrich (Saint Louis, USA) with an excitation/emission: 358
124 nm/ 410 nm. Commercial nanoplastics are suspended in ultrapure water with Tween-
125 20© surfactant (<0.1%) to limit aggregation (Sigma-Aldrich). Before exposure, NP
126 were vortexed to prevent particle aggregation and insure good suspension
127 homogenization before use. An intermediate solution was prepared in ultrapure water
128 (concentration of 1 mg mL⁻¹) and a final volume of 1.5 mL of NP were add to a final
129 volume of 300 mL of culture that was kept in continuous aeration to ensure good
130 dispersion. Final concentration of Tween-20© in the cultures were < 0.00002% in the
131 higher NP treatment. Non-ionic surfactants had previously been demonstrated to be
132 innocuous for marine microalgae at this dose (Pavlic et al., 2005) so no effect is
133 expected owing to its residual concentration in all samples (Douglas et al., 1985). For
134 each batch culture (stationary and exponential), three experimental treatments were
135 tested: control (no NP), low NP concentration (0.05 $\mu\text{g mL}^{-1}$) and high NP
136 concentration (5 $\mu\text{g mL}^{-1}$). All treatments (control, low and high) were performed in

137 triplicates for each growth phase (exponential and stationary) and microalgae were
138 exposed for 96 hours. NP characteristics were determined by Dynamic light scattering
139 (DLS) in ultrapure water and in filtered spent media of algae cultures as described in
140 González-Fernández et al. (2019). NP resuspended in ultrapure water and seawater
141 showed expected sizes (50 nm) and no aggregation ($PdI < 0.2$). NP size and aggregation
142 state monitored in the filtered spent media of algae cultures revealed a moderate
143 aggregation, showing a size of 70.5 ± 2.2 nm ($PdI > 0.2$) and 162.4 ± 3.3 nm ($PdI >$
144 0.2) for exponential and stationary media respectively.

145 2.2. Analyses

146 2.2.1. Pigments extraction and composition

147 At the end of the experiment, 3.5 mL and 25 mL corresponding to a total of 2×10^7 cells
148 of diatom cultures at exponential and stationary phases were filtered over glass fiber
149 filters (preliminary burned for 6 h at 450 °C; 0.2 μ m, Whatman GF/F) and stored at -80
150 °C. Pigments were then extracted in methanol and analyzed by HPLC (Ras et al., 2008).
151 All the pigment standards were purchased from DHI (HØRSHOLM, Denmark). A total
152 of 11 pigments were identified at both growth phases: chlorophyll a (Chl *a*) and sub-
153 products of chlorophyll a (allo and epi Chl *a*), chlorophyll c (Chl *c2*), fucoxanthin (Fx),
154 β -carotene (β -car), diadinoxanthin (Ddx), diatoxanthin (Dtx), violaxanthin (Vx),
155 neoxanthin (Nx) and pheophytin (Phx).

156 2.2.2. Lipid class and fatty acid analyses

157 For lipid class and fatty acid analyses, 4×10^7 cells (7 mL of exponential cultures and
158 50 mL of stationary cultures) were filtered over glass fiber filters (preliminary burned
159 for 6 h at 450 °C; 0.2 μ m, Whatman GF/F). Boiling water was immediately passed
160 through the filter after filtration to inhibit lipase activity and prevent lipid degradation.

161 Lipids were then extracted with chloroform:methanol (2:1; v:v). Lipid extracts were
162 stored at $-20\text{ }^{\circ}\text{C}$ under nitrogen (N_2 (g)) until analysis. Lipid class analyses were
163 performed by high-performance thin layer chromatography (HPTLC) using a CAMAG
164 auto-sampler to spot the sample on HPTLC glass plates pre-coated with silica gel
165 (Merck & Co., Ltd., Darmstadt, Germany). In *C.neogracile* cultures, the following lipid
166 classes were measured: within the phospholipids (phosphatidylinositol (PI),
167 phosphatidyl choline (PC) and Phosphatidylserine (PS)), within the glycolipids
168 (monogalactosyl-diacylglycerol (MGDG) and digalactosyl-diacylglycerol (DGDG)),
169 globally the sum of phosphatidyl ethanolamine (PE), phosphatidyl glycerol (PG) and
170 sulfoquinovosyl-diacylglycerol (SQDG), free sterols (FST), free fatty acids (FFA) and
171 triglycerides (TAG).

172 In this study, neutral lipid (NL) classes, which mostly contains the reserve lipids and
173 polar lipid (PL) classes, which contains most of the membrane lipids, were analyzed
174 (Moutel et al., 2016). For polar and neutral lipid fatty acid (FA) analysis, an aliquot of
175 the lipid extract was dried under N_2 (g) and then resuspended in chloroform:methanol
176 (98:2; v:v). Separation of neutral and polar lipids was realized by solid phase
177 extraction (Le Grand et al., 2013). Each fraction (PL and NL) was then dried under N_2
178 (g) and transesterified. The resulting fatty acid methyl esters (FAME) were analyzed
179 and quantified by gas chromatography (GC-FID) (Le Grand et al., 2013) and FA
180 identification controlled using standards (Long et al., 2018). FA compositions were
181 expressed as relative mass percentage of total FA in PL and NL. Fatty acids of diatoms
182 at both growth phases with values higher than zero are listed in supplementary Tables 1
183 and 2. Two fatty acids iso-15:0 and iso-17:0, specific markers of prokaryote presence
184 (Suroy et al., 2014a) were identified, but they were excluded from analysis due to they
185 are not specific markers of diatoms.

186 2.2.3. Lipid reserves monitoring by flow cytometry

187 Changes of in the reserve cell content after 96 h exposure to NP were monitored using a
188 green-fluorescent dye (BODIPY 505/515 FL; Thermo Fisher scientific). BODIPY can
189 be used as a proxy of lipid reserves as it stains lipid droplets (Govender et al., 2012).
190 We validated that, presence of NP, did not interfere the measurement of BODIPY in
191 algae. Samples were incubated with BODIPY at a final concentration of 10 mM for 10
192 min at 18 °C in the dark. Analysis were performed for 30 sec at 0.12 $\mu\text{l sec}^{-1}$ flow rate
193 using an EasyCyte Plus cytometer (Guava Technologies, Millipore, Billerica, MA).
194 Additionally, culture cell concentration (cell mL^{-1}) was recorded during analysis.
195 Results were expressed in arbitrary units (A.U).

196 2.3. Statistical analyses

197 Statistical analysis of pigment composition and main lipid classes were performed using
198 STATGRAPHICS centurion XV.II (Statpoint Technologies, Inc. Warrenton, Virginia,
199 USA). Data normality and homogeneity of variances were tested. Student's t-test was
200 used to compare variables between exponential vs. stationary phases. For each culture
201 phase, one-way-ANOVA analysis was performed to establish significant differences
202 between treatments (control, low and high) using a Tukey's post hoc test to differentiate
203 treatments. A simple regression analysis was used to link cellular responses already
204 reported in this cells (González-Fernández et al., 2019) and results from the present
205 study. Differences were considered significant at $p < 0.05$.

206 Fatty acid data were statistically analyzed using PRIMER.V6 with a similarity
207 percentage analysis (*SIMPER*) being performed on the relative FA percentage data to
208 demonstrate the differences in FA according to growth phases. Only FA showing values
209 higher than 0.5 were included in the analysis. *SIMPER* identifies the FA that contribute

210 most to the variations in the assemblage patterns recorded. The FA that cumulatively
211 contributed up to 80% of the dissimilarities recorded were selected to characterize the
212 differences in the FA profile of *C. neogracile* at different growing phases. Due to
213 significant differences of the FA profile in *C. neogracile* at exponential and stationary
214 phases, analysis of NP effects were performed independently for each growth phase.

215 For analysis, data on the relative FA percentages of the samples were $(\log [x + 1])$
216 transformed and converted into a *Bray-Curtis* similarity matrix to start the multivariate
217 analyses. Later, the Bray-Curtis similarity matrix was used for one-way ANOSIM to
218 test whether algae exposed to NP (within NL or PL fractions) were significantly
219 clustered according to exposure treatments. ANOSIM calculates a global R statistic that
220 assesses the differences between groups, with $R = 1$, $R = 0.5$ and $R = 0$ indicating a
221 perfect, satisfactory and poor separation of the clusters, respectively (Clarke et al.,
222 2008).

223 Principal component analysis (PCA) was carried out in order to establish relationships
224 between treatments and individual FA. For this study, the components whose
225 cumulative variance explained $> 60\%$ of variance were considered.

226 **3. Results**

227 3.1. Pigment and lipid compositions of *C. neogracile* according to growth phase

228 Pigment composition of *C. neogracile* at the two different growth phases is presented in
229 Table 1. Significant differences in all pigment cell contents were observed between
230 exponential and stationary phases (*T-student test*; $p < 0.001$ all cases) presenting higher
231 values at exponential phase.

232 Significantly higher total lipid concentration per cell were observed at stationary phase
233 than at exponential phase (*T-student test*; $p < 0.05$; Supplementary Figure 1) mainly due

234 to differences in reserve lipids (TAG, *T-student test*; $p<0.001$). Significantly higher
235 content of DGDG and FST were also observed at stationary phase compared to
236 exponential phase (Supp. Figure 2).

237 Furthermore, influence of growth phase on FA composition of polar and neutral lipids
238 was also investigated (Supp. Tables 1 and 2, respectively). At exponential phase, higher
239 proportions of polyunsaturated fatty acids (PUFA) were observed compared to
240 stationary phase for both lipid fractions (*T-student test*; $p<0.01$). A very good separation
241 of FA between growing phases was observed in both lipid fractions: polar lipids'
242 composition (*Stress*=0.00, NMDS) and neutral lipids' composition (*Stress*=0.00,
243 NMDS). The main differences observed came from SFA (such as 14:0, 16:0 and 18:0),
244 MUFA (18:1n-7; 18:1n-9, 18:1n-5) and PUFA (20:5n-3; 16:2n-7; 16:3n-4; 22:6n-3 and
245 20:4n-6) showing a dissimilarity between growth phases of 19.7% and 19.8% for polar
246 and neutral lipids, respectively (*SIMPER* analysis).

247 3.2. Changes in pigment and lipid compositions after exposure to NP

248 At exponential phase, a decrease (-75%) in the quantity of pigments composing the
249 fucoxanthin-chlorophyll protein (FCP) complex was observed upon high NP exposure:
250 Chl *c*2, Chl *a* and sub-products allo and epi Chl *a* as well as Fx (Table 1). Additionally,
251 a significant reduction of β -car and Phx (-63.7% and -75.5% respectively) in this
252 condition was observed whereas the ratio Dtx/Ddx increased (+1316% equivalent to 13
253 times higher than controls). At stationary phase, Chl *c*2, β -car and Phx were
254 significantly reduced by both NP concentrations (Table 1).

255 When analyzing lipid classes by HPTLC, a decrease in DGDG and MGDG cell content
256 (-28.5% and -46.1%, respectively) was observed in exponential cultures after exposure
257 to high NP concentration (Figure 1A). Moreover, a reduction of the ratio

258 MGDG/DGDG (-24.8%) was observed (Figure 2) at high NP exposure. The meantime,
259 increases of PS (+41.7%) and FFA (+242%) cell contents were observed at high NP
260 concentrations as well as increase of TAG (+77.6% and +53.3%) at low and high NP
261 exposures, respectively (Fig. 1A). *C. neogracile* at stationary phase showed significant
262 increases of MGDG and TAG (+45.4% and +34.7%, respectively) at high NP
263 concentration (Figure 1B). A dose-dependent increase in the ratio MGDG/DGDG was
264 also observed (Figure 2).

265 Additionally, neutral lipid content of cells was measured by flow cytometry after 96 h
266 exposure to NP using BODIPY staining (Figure 3). At exponential phase, lipid reserves
267 were increased at low but not at high NP concentration. Conversely, at stationary phase
268 a dose-response increase of lipid reserves was observed upon NP exposure (Fig. 3).

269 3.3. Changes in FA profiles after exposure to nanoplastics

270 Changes in their FA profile after exposure to the NP concentration was evidenced at
271 exponential growth (Figure 4). In the PL fraction, differences were observed after
272 exposure to high NP concentration (Global $R=0.8$, $p<0.01$; *ANOSIM*) but not at low
273 concentration. The main FA responsible for differences between control and high NP
274 exposure were: 18:1n-7 (accounting for 22.8% of the dissimilarity); 22:6n-3 (7.8%);
275 18:2n-6 (7.4%); 18:0 (7.0%); 18:4n-3 (5.6%); 16:1n-7 (5.0%); 16:2n-7 (4.5%); 16:0
276 (4.0%); 16:3n-4 (3.7%); 18:3n-6 (3.5%); 16:2n-4 (3.5%); 20:4n-6 (3.4%) and 18:1n-9
277 (3.2%), accounting together for 81.5% of dissimilarity (*SIMPER* analysis; $DS=7.02$).

278 Significant differences were also evidenced in NL fraction at both NP concentrations
279 (Global $R=1$, $p<0.01$; *ANOSIM*). Differences between control and low NP exposure
280 were associated to the percentage of 16:2n-6 (accounting for 15.9% of the
281 dissimilarity); 16:4n-3 (13.3%); 18:0 (10.6%); 16:1n-9 (6.6%); 18:1n-9 (6.3%); 18:4n-3

282 (5.9%); 16:1n-7 (5.5%); 14:1n-5 (4.5%); 18:3n-6 (4.1%); 16:0 (3.0%); 14:0 (2.8%) and
283 16:2n-4 (2.7%) accounting for the 81.2% of dissimilarity (*SIMPER* analysis; DS=6.80).
284 Differences between control and high NP exposure were determined by the percentage
285 of 16:3n-4 (accounting for 15.3% of dissimilarity); 16:2n-6 (11.9%); 16:4n-3 (8.5%);
286 16:0 (7.1%); 16:2n-7 (5.2%); 16:2n-4 (5.1%); 18:0 (4.8%); 18:2n-6 (4.5%); 20:4n-6
287 (4.2%); 14:1n-5 (4.2%); 16:1n-7 (3.7%); 16:1n-9 (3.6%) and 18:1n-9 (3.2%) accounting
288 for the 81.4% of dissimilarity (*SIMPER* analysis; DS=7.94).

289 In the PL fraction, the 2 first principal components of the PCA explained 86% of the
290 variability in the original data, respectively explaining 50.7% and 34.8% of the
291 combined variance. The representation of PC1 and PC2 (Fig. 4A) distinguished an
292 increase in the proportions of 18:0, 18:1n-7, 16:2n-7, 16:2n-4, 16:3n-4 and 22:6n-3 at
293 high NP concentration while 16:0, 16:1n-7, 18:1n-9, 18:2n-6, 18:3n-6, 18:4n-3 and
294 20:4n-6 decreased at this condition showing higher values at control and low NP
295 exposure treatments (Fig. 4A; 4B).

296 In the NL fraction, the PC1 and PC2 explained respectively 48% and 38.9% of the total
297 variance (Fig. 4C). PC1 separate low and high NP exposures while PC2 revealed
298 differences between control and NP exposed treatments. The PC1-PC2 factorial plan
299 (Fig. 4D) distinguished an increase in the proportions of 16:2n-6, 18:1n-9 and 20:4n-6
300 in control compare to NP treatments. Cultures exposed to high NP concentrations
301 evidenced higher proportions of 16:0, 18:0, 16:2n-7, 16:2n-4 and 16:3n-4 while culture
302 exposed to low NP concentrations was characterized by higher proportions of 14:0,
303 14:1n-5, 16:1n-7, 18:3n-6 and 18:4n-3. The rest of FA that accounted for >80%
304 differences between treatments was not determinant to establish differences between
305 control and NP exposures due to the low factor loading obtained (<0.1).

306 At stationary growth, no significant differences between treatments were observed in
307 both lipid fractions analyzed.

308 **4. Discussion:**

309 **Characterization of pigment and lipid composition of *C. neogracile***

310 In general and in our study, most of the pigments in diatoms showed lower cellular
311 concentrations during stationary growth and the senescence, particularly, the light-
312 harvesting pigments Chl *a* and sub-products, Chl *c*2, Fx and β -car, as a result of
313 nutritional limitations in the media (Carreto and Catoggio, 1976; Klein, 1988;
314 Kuczynska et al., 2015). We observed accumulation of triacylglycerol (TAG) at
315 stationary phase, a general response of diatoms to nutrient limitation (Li et al., 2014;
316 Pratiwi et al., 2009). FA acid composition of *C. neogracile*, showed high proportions of
317 14:0, 16:0: 16:1n-7, 20:4n-6, 20:5n-3 (EPA) and 22:6n-3 (DHA), characteristic of
318 diatoms (González-Fernández et al., 2016; Zulu et al., 2018). In the present study,
319 proportions of SFA and MUFA increased while the proportion of PUFA decreased
320 during stationary phase. Nutrient limitation promotes re-adjustment of lipid
321 compartment. SFA and MUFA increase at the cost of PUFA under phosphate limitation,
322 possibly in relation to the need for NADP during desaturation and elongation
323 (Jónasdóttir, 2019). We previously demonstrated that culture age influences the impact
324 of NP, indicating higher cellular toxicity at exponential growth phase than at stationary
325 phase (González-Fernández et al., 2019). As a continuation of this work, we evaluated
326 lipid composition of diatoms at exponential and stationary growth phases exposed to
327 two NP concentrations (0.05 and 5 $\mu\text{g mL}^{-1}$).

328 **Impairment of the photosynthetic machinery after exposure to NP**

329 In the aquatic environment, pigments may undergo degradation in response to chemical,
330 photochemical and biological processes being chlorophylls the most labile compounds
331 (Zigmantas et al., 2004). Changes in photosynthetic pigment levels are usually a fast
332 response to stressful conditions because they are engaged in basic processes such as
333 photosynthesis and photoprotection essential for cell life (Kuczynska et al., 2015). Our
334 results reveal a drastic impact of NP on the photosynthetic machinery of diatoms. The
335 concentrations of pigments associated with the fucoxanthin-chlorophyll protein (FCP)
336 complexes (Chl *a*, Chl *c*2 and Fx) were significantly reduced after exposure to high NP
337 concentration in exponential cultures. The decrease in photosynthetic efficiency in this
338 cells were previously observed upon 96 h exposure to $0.05 \mu\text{g mL}^{-1}$ and $5 \mu\text{g mL}^{-1}$ NP
339 (González-Fernández et al., 2019) and showed a close positive relationship with the
340 decrease of Chl *a* observed in this study (Regression, $R^2=0.89$, $p<0.05$). The decrease of
341 photosynthetic efficiency may result from an inactivation of photosystem (PSII)
342 (Lelong et al., 2011). Thus, photons become excessive and may induce an increase in
343 ROS production by the cell. To avoid this, algae have developed photo-protective
344 mechanisms such as non-photochemical quenching (NPQ) as well as the activation of
345 the xanthophyll cycle (Kuczynska et al., 2015). Diadinoxanthin (Ddx) and diatoxanthin
346 (Dtx) are the main xanthophyll cycle pigments (Grouneva et al., 2009). In the present
347 study, an increase of Dtx at the expense of Ddx (Dtx/Ddx ratio) was observed upon
348 exposure to NP at exponential growth. The deepoxidation of Ddx to Dtx is an essential
349 prerequisite of the thermal dissipation of excess excitation energy and it is considered
350 the most important photoprotective mechanism in diatoms (Goss and Jakob, 2010;
351 Lavaud et al., 2007). Using simple regression, Dtx/Ddx ratio had a positive linear
352 relationship with ROS production at exponential stage ($R^2= 0.43$, $p<0.05$). It seems that

353 diatoms at this stage used NPQ strategy to dissipate the excess of energy produced by
354 NP presence.

355 At stationary phase, only few pigments were impacted by NP exposure: β -car which is
356 one of the main photo-protective carotenoids, Chl *c2* that participates effectively in
357 photosynthesis as an accessory pigment (Kuczynska et al., 2015) and Phx which
358 derivate of chlorophyll and has been recently identified as the primary electron acceptor
359 of PSII (Klimov, 2014). Nevertheless, the decrease observed on pigment composition
360 upon NP exposure highlights that diatoms are susceptible to NP exposure also at
361 stationary phase.

362 **NP modulates thylakoid and membrane lipid composition**

363 Analysis of lipid classes revealed that NP exposure impacted proportions and ratios of
364 MGDG and DGDG, which are the main constituents of thylakoid membranes,
365 accounting for about 50 and 25% of total thylakoid lipids, respectively (Dorney, 2013).
366 Surprisingly, MGDG/DGDG ratio of cells at exponential and stationary growth changed
367 in opposite direction in a dose-dependent manner upon exposure to NP. Fluctuations in
368 the MGDG/DGDG ratio could affect the properties and structures of thylakoid
369 membranes by altering the lipid organization from hexagonal inverse to lamellar phases
370 (Dorney, 2013). Thylakoid lipids not only provide a lipid bilayer matrix but also form
371 part of the structural components in PSII and photosystem I (PSI) complexes
372 (Kobayashi, 2018). The deepoxidation of Ddx occurs in presence of MGDG (Goss et
373 al., 2007). Decreases in the MGDG cell content observed in exponential cultures upon
374 NP exposure suggest that MGDG has been used for Ddx deepoxidation. The re-
375 arrangement of thylakoid lipid composition can be related to the maintenance of
376 functional chloroplasts preventing photo-oxidative damage from intermediate

377 complexes or unbalanced electron transfer systems (Fujii et al., 2014). Thus, we can
378 speculate that MGDG are being used by cells to reduce superoxide radicals accumulated
379 in cells (Kuczynska et al., 2015) as consequence of NP presence, as previously
380 discussed in (González-Fernández et al., 2019).

381 On the other hand, increase in MGDG/DGDG ratio was observed upon NP exposure at
382 stationary phase that may indicate changes in thylakoid membrane' structure. Changes
383 in membranes of microalgae' cells under MP exposure have been previously reported
384 showing a thickening of algal cell walls, which could effectively block the invasion of
385 MP and thus avoid cell damage (Mao et al., 2018).

386 Changes in membrane fatty acid (FA) profile upon NP exposure were also observed. In
387 exponential phase, at high NP concentration, an increase in proportions of polar lipid
388 FA 18:1n-7, 16:2n-4, 16:3n-4 at the expenses of 16:0, 18:2n-6, 18:3n-6, 18:4n-3 and
389 20:4n-6 suggested some metabolic responses/adjustments in PUFA pathways.
390 Synthesis of the n-7 and n-4 PUFA series occur in chloroplast and used 16:1n-7 as
391 precursor while n-3 and n-6 synthesis may occur from 16:0 in chloroplast and 18:0 in
392 chloroplast and endoplasmic reticulum synthesized through fatty acid synthase (Liang et
393 al., 2013). The synthesis of *de novo* FA and galactolipids is linked with photosynthetic
394 electron transport of chloroplasts. The reduction observed at exponential phase of
395 MGDG and DGDG could impair the PSII photochemical reaction and disrupt energy
396 coupling between reaction centers and antenna complexes (Fujii et al., 2014). Since
397 MGDG and DGDG from diatoms are synthesised in the "prokaryotic" pathway, and are
398 enriched in 16-carbons fatty acids in the sn-2 position (Bromke et al., 2015), a
399 significant reduction of MGDG and DGDG may result in changes of fatty acid
400 biosynthesis and metabolism (Zulu et al., 2018). Similar changes of PUFA have been
401 previously revealed after algae exposure to pesticides (Filimonova et al., 2016)

402 decreasing the level of 18:2, 18:3 but increasing the level of EPA (20:5n-3) and MUFA
403 (16:1 and 18:1) (Filimonova et al., 2016).

404 Moreover, the decrease in 14:0 and 16:0 at high NP concentration may reflect some
405 changes in cell' frustules as these two FA were identified as main saturated FA
406 conforming diatoms' frustule-associated lipid fractions (Suroy et al., 2014b). The
407 attachment of 50 nm PS-NH₂ to diatoms cell' frustules has been previously
408 demonstrated by scanning electron micrographs (SEM) at exponential phase (González-
409 Fernández et al., 2019). In addition, absorption of PS-NH₂ NP on algae' cell membranes
410 has been also reported in green algae (Bergami et al., 2017; Nolte et al., 2017).
411 Nevertheless, the presence of a silica frustule in diatoms could protect from the negative
412 effects of NP in membranes. It has been reported that -NH₂ have high affinity to
413 frustule's silica in diatoms (Walsh et al., 2017). In this sense, although the impact of NP
414 on diatoms' frustule has not been identified yet, the attachment of NP to frustules could
415 reduce light availability and nutrient and gas exchange, potentially impacting the
416 photosynthesis activity (González-Fernández et al., 2019) and affecting its machinery as
417 reported above (the decrease in FCP pigments and activation of Ddx cycle).

418 Contrary to the effect observed at exponential phase, membrane lipid composition was
419 not affected by NP at stationary phase. Cultures at stationary phase present 6 times
420 higher TEP concentration by cell than at exponential phase (González-Fernández et al.,
421 2019). Presence of TEP in culture media act as an adhesive, binding particles together
422 (Summers et al., 2018) increasing aggregation. This aggregation promotes the increase
423 of NP size and may reduce their associated impacts. Secondly, cells at exponential
424 phase are more susceptible to stress due to the fast growth which requires energy and
425 promote membrane exhibition (Tanaka et al., 2015).

426 Readjustment of lipid reserves upon NP exposure

427 The increase in reserve lipids in microalgae is an acclimation mechanism to cope with
428 the decrease of nutrient availability or the presence of anthropogenic pollution
429 (Guschina and Harwood, 2006). In our study, cells exposed to NP concentration
430 displayed higher TAG than non-exposed cells. TAG increased not only after exposure
431 to high NP concentration but also upon low NP concentration. This fact, indicates that
432 lipid measurements are sensitive enough to evaluate the impact of NP exposure even at
433 environmental concentrations. TAG can be temporarily stock-piled in essentially
434 unlimited amounts and be utilized as an energy-rich carbon source when favorable
435 conditions come back. Some algal species make dual use of excess lipid stores, both as
436 a reserve for future growth and as a mean of reducing photosynthesis by directly
437 absorbing part of the incoming light (Thompson, 1996). The reduction of content of
438 principal pigments associated to light-harvesting functions observed in exponential
439 cultures, together with the accumulation of ROS previously observed (González-
440 Fernández et al., 2019) may result in promoting the accumulation of TAG for survival
441 at both growth phases.

442 In addition to that, fatty acid composition of reserve lipids were also affected by NP
443 exposure at both concentrations. However, fatty acid re-arrangement differed according
444 to the concentration of NP used. Some of the changes observed in cultures exposed to
445 high NP concentration may be related to the impairment of long chain fatty acids
446 synthesis by affecting the fatty acid elongase and therefore reducing the proportion of
447 C18 and C20 fatty acids (the conventional pathway to EPA) (Filimonova et al., 2016).
448 As consequence of this interference, an accumulation of precursors of the fatty acid
449 elongase, 16:0 was observed(Filimonova et al., 2016). Most of microalgae naturally
450 synthesize significant quantity of free fatty acids (FFA) that are further converted to

451 acyl-CoA thioesters for lipid biosynthesis and accumulation (Hao et al., 2018).
452 Nevertheless, interruption of fatty acid elongation cycle can promote the release of FFA
453 as observed in our study in cultures exposed to high NP exposure.

454 Cultures exposed to low NP concentration also evidenced a high percentage of 16:1n-7.
455 Desaturation steps starting from 16:1n-7 are linked with the glycerol-backbone of
456 galactolipids, usually MGDG (Zulu et al., 2018). Although MGDG were not affected at
457 this low NP concentration, the ratio MGDG/DGDG showed a dose-dependent reduction
458 with NP concentration. This may serve as an alternative way to compensate the decrease
459 of C18-20 PUFA observed at upon NP exposure. Particular attention should be drawn to
460 the 16:2n-6 and 16:3n-4 fatty acids, which were PUFA determinant for the
461 discrimination of control and NP exposed cultures. In diatoms, plastidial desaturases
462 have been identified as enzymes involved in the generation of 16:3n-4, which represents
463 an unusual Δ^6 -harboring C16-PUFA (Zulu et al., 2018). The incorporation of some
464 PUFA into TAG may result from membrane lipid remodeling by the release of PUFA
465 from galactolipids (Zulu et al., 2018). The increase of TAG at low and high NP
466 exposure, together with the decrease of MGDG/DGDG ratio observed upon exposure to
467 NP in exponential cultures may suggest a major readjustment of lipids to cope the stress
468 exerted by NP.

469 In this work, we measured TAG concentration through HPTLC. Additionally, we
470 monitored changes in the reserve cell content after 96 h exposure to NP by flow
471 cytometry, using a fluorescent dye (BODIPY). Our results showed that measurements
472 of lipid reserves by flow cytometry and HPTLC displayed the same tendency being a
473 good indicator of lipid reserves in algae. These results are of great interest not only for
474 laboratories studies but also for field works since it is a fast and economic measurement
475 that will provide a proxy of the energetic status of the microalgae. This technique

476 revealed high sensitivity to detect reserve lipid changes in cells even upon potential
477 environmental concentrations of NP being a good indicator of environmental stress.

478 **5. Conclusion**

479 In conclusion, our results bring new insights of NP effects on diatoms and indicate how
480 NP impair their photosynthetic machinery and affect lipid structures. Diatoms' pigment
481 cell content was drastically reduced upon NP exposure at both physiological states
482 evidencing the impact of NP mainly on the FCP associated pigments at both
483 concentrations. A readjustment of thylakoid' lipid class and fatty acid compositions was
484 also induced by NP exposure. Interestingly, although the impact of NP on diatoms was
485 dependent of culture growth, being more sensitive at exponential culture than at
486 stationary one, cells in different physiological phases were able to develop different
487 acclimation mechanisms to cope with the NP induced stress. Altogether, compositions
488 of reserve and membrane lipids are new and sensitive markers to assess the impact of
489 NP exposure, including at low dose, on marine organisms. Finally, we validated the
490 measurement of reserve lipid content in cells by flow cytometry as a tool for identifying
491 changes associated to lipid reserves in diatoms.

492 **Acknowledgements**

493 The authors thank P. Miner and A. Donval, staffs of the Ifremer facilities in Plouzané
494 for their help in production and maintenance of diatoms' cultures as well as pigment
495 composition analyses. We are particularly grateful to N. Le Goïc and C. Lambert for
496 their technical assistance during the experiment. This work was supported by the
497 NANO Project (ANR-15-CE34-0006-02) funded by the French Agence Nationale de la
498 Recherche (ANR), by the Unique Inter-ministerial Fund (FUI) and the local
499 communities (CR Bretagne, CR PACA, CD29, CATPM and Brest Metropole) as part of

500 the MICROPLASTIC2 project (Region Bretagne 0214/15008381/00001897, Bpifrance
501 D0S0028206/00) and the project SAD 2015 - IN MEMO (#9245) funded by the
502 Brittany Region within the SAD “Stratégie Attractivité Durable” strategy.

503 **References**

504 Al-sid-cheikh, M., Rowland, S.J., Stevenson, K., Rouleau, C., Henry, T.B., Thompson,
505 R.C., 2018. Uptake, Whole-Body Distribution, and Depuration of Nanoplastics by
506 the Scallop *Pecten maximus* at Environmentally Realistic Concentrations. Environ.
507 Sci. Technol. 52, 14480–14486. <https://doi.org/10.1021/acs.est.8b05266>

508 Amaral-Zettler, L., Andrady, A., Dudas, S., Fabres, J., Galgani, F., Hardesty, D.,
509 Hidalgo-Ruz, V., Hong, S., Kershaw, P., Lebreton, L., Lusher, A., Narayan, R.,
510 Pahl, S., Potemra, J., Rochman, C., Sherif, S.A., Seager, J., Shim, W.J., Sobral, P.,
511 Takada, S., Brink, P. ten, Thiel, M., Thompson, R., Turra, A., Cauwenberghe, L.
512 Van, Sebille, E. van, Vethaak, D., Watkins, E., Wyles, K., Wilcox, C., Zettler, E.,
513 Ziveri, P., 2016. Sources, fate and effects of microplastics in the marine
514 environment: Part 2 of a global assessment. Reports Stud. GESAMP 93, 217.
515 <https://doi.org/10.13140/RG.2.1.3803.7925>

516 Avio, C.G., Gorbi, S., Milan, M., Benedetti, M., Fattorini, D., D’Errico, G., Pauletto,
517 M., Bargelloni, L., Regoli, F., 2015. Pollutants bioavailability and toxicological
518 risk from microplastics to marine mussels. Environ. Pollut. 198, 211–222.
519 <https://doi.org/10.1016/j.envpol.2014.12.021>

520 Balbi, T., Camisassi, G., Montagna, M., Fabbri, R., Franzellitti, S., Carbone, C.,
521 Dawson, K., Canesi, L., 2017. Impact of cationic polystyrene nanoparticles (PS-
522 NH₂) on early embryo development of *Mytilus galloprovincialis*: Effects on shell
523 formation. Chemosphere 186, 1–9.

- 524 <https://doi.org/10.1016/j.chemosphere.2017.07.120>
- 525 Bergami, E., Pugnali, S., Vannuccini, M.L., Manfra, L., Faleri, C., Savorelli, F.,
526 Dawson, K.A., Corsi, I., 2017. Long-term toxicity of surface-charged polystyrene
527 nanoplastics to marine planktonic species *Dunaliella tertiolecta* and *Artemia*
528 *franciscana*. *Aquat. Toxicol.* 189, 159–169.
529 <https://doi.org/10.1016/j.aquatox.2017.06.008>
- 530 Bergmann, M., Gutow, L., Klages, M., Bergmann, M., Klages, M., 2015. Marine
531 anthropogenic litter. *Mar. Anthropol. Litter* 1–447. [https://doi.org/10.1007/978-3-](https://doi.org/10.1007/978-3-319-16510-3)
532 [319-16510-3](https://doi.org/10.1007/978-3-319-16510-3)
- 533 Bhattacharya, P., Lin, S., Turner, J.P., Ke, P.C., 2010. Physical adsorption of charged
534 plastic nanoparticles affects algal photosynthesis. *J. Phys. Chem. C* 114, 16556–
535 16561. <https://doi.org/10.1021/jp1054759>
- 536 Bromke, M.A., Sabir, J.S., Alfassi, F.A., Hajarrah, N.H., 2015. Metabolomic Profiling of
537 13 Diatom Cultures and Their Adaptation to Nitrate-Limited Growth Conditions
538 1–17. <https://doi.org/10.1371/journal.pone.0138965> Carreto, J.I., Catoggio, J.A.,
539 1976. Variations in pigment contents of the diatom *Phaeodactylum tricornutum*
540 during growth. *Mar. Biol.* 36, 105–112. <https://doi.org/10.1007/BF00388433>
- 541 Clarke, K.R., Somerfield, P.J., Gorley, R.N., 2008. Testing of null hypotheses in
542 exploratory community analyses: similarity profiles and biota-environment
543 linkage. *J. Exp. Mar. Bio. Ecol.* 366, 56–69.
544 <https://doi.org/10.1016/J.JEMBE.2008.07.009>
- 545 Della Torre, C., Bergami, E., Salvati, A., Faleri, C., Cirino, P., Dawson, K.A., Corsi, I.,
546 2014. Accumulation and Embryotoxicity of Polystyrene Nanoparticles at Early
547 Stage of Development of Sea Urchin Embryos *Paracentrotus lividus*. *Environ. Sci.*

- 548 Technol. 48
- 549 Dolch, L.J., Marechal, E., 2015. Inventory of fatty acid desaturases in the pennate
550 diatom *Phaeodactylum tricornutum*. Mar. Drugs 13, 1317–1339.
551 <https://doi.org/10.3390/md13031317>
- 552 Dorney, J., 2013. Polystyrene : A Potential Standard for Developing *In Vitro* Cellular
553 Tracking Methods for Nanotoxicology. <https://doi.org/10.21427/D75C76>
- 554 Douglas, S.J., Illum, L., Davis, S.S., 1985. Particle size and size distribution of poly
555 (butyl 2-cyanoacrylate) nanoparticles. II. Influence of stabilizers. J. Colloid
556 Interface Sci. 103 (1), 154-163.
- 557 Fotopoulou, K.N., Karapanagioti, H.K., 2012. Surface properties of beached plastics.
558 Mar. Environ. Res. 81, 70–77. <https://doi.org/10.1007/s11356-015-4332-y>
- 559 Filimonova, V., Gonçalves, F., Marques, J.C., De Troch, M., Gonçalves, A.M.M., 2016.
560 Fatty acid profiling as bioindicator of chemical stress in marine organisms: A
561 review. Ecol. Indic. 67, 657–672. <https://doi.org/10.1016/j.ecolind.2016.03.044>
- 562 Fujii, S., Kobayashi, K., Nakamura, Y., Wada, H., 2014. Inducible knockdown of
563 Monogalactosyldiaculglycerol Synthase1 reveals roles of galactolipids in organelle
564 differentiation in *Arabidopsis Cotyledons*. Plant Physiol. 166, 1436–1449.
565 <https://doi.org/10.1104/pp.114.250050>
- 566 Galloway, T.S., Cole, M., Lewis, C., 2017. Interactions of microplastic debris
567 throughout the marine ecosystem. Nat. Ecol. Evol. 1, 1-16.
568 <https://doi.org/10.1038/s41559-017-0116>
- 569 González-Fernández, C., Lacroix, C., Paul-Pont, I., Le Grand, F., Albentosa, M., Bellas,
570 J., Viñas, L., Campillo, J.A., Hegaret, H., Soudant, P., 2016. Effect of diet quality

- 571 on mussel biomarker responses to pollutants. *Aquat. Toxicol.* 177, 211–225.
572 <https://doi.org/10.1016/j.aquatox.2016.05.027>
- 573 González-Fernández, C., Toullec, J., Lambert, C., Le Goïc, N., Seoane, M., Moriceau,
574 B., Huvet, A., Berchel, M., Vincent, D., Courcot, L., Soudant, P., Paul-Pont, I.,
575 2019. Do transparent exopolymeric particles (TEP) affect the toxicity of
576 nanoplastics on *Chaetoceros neogracile*? *Environ. Pollut.* 250, 873–882.
577 <https://doi.org/10.1016/j.envpol.2019.04.093>
- 578 Goss, R., Latowski, D., Grzyb, J., Vieler, A., Lohr, M., Wilhelm, C., Strzalka, K. 2007.
579 Lipid dependence of diadinoxanthin solubilization and deepoxidation in artificial
580 membrane systems resembling the lipid composition of the natural thylakoid
581 membrane. *Biochim. Biophys. Acta.* 1768, 67–75.
- 582 Goss, R., Jakob, T., 2010. Regulation and function of xanthophyll cycle-dependent
583 photoprotection in algae. *Photosynth. Res.* 106, 103–22.
584 <https://doi.org/10.1007/s11120-010-9536-x>
- 585 Govender, T., Ramanna, L., Rawat, I., Bux, F., 2012. BODIPY staining, an alternative
586 to the Nile Red fluorescence method for the evaluation of intracellular lipids in
587 microalgae. *Bioresour. Technol.* 114, 507–511.
588 <https://doi.org/10.1016/j.biortech.2012.03.024>
- 589 Grouneva, I., Jakob, T., Wilhelm, C., Goss, R., 2009. The regulation of xanthophyll
590 cycle activity and of non-photochemical fluorescence quenching by two alternative
591 electron flows in the diatoms *Phaeodactylum tricornutum* and *Cyclotella*
592 *meneghiniana*. *Biochim. Biophys. Acta - Bioenerg.* 1787, 929–938.
593 <https://doi.org/10.1016/J.BBABIO.2009.02.004>
- 594 Guschina, I.A., Harwood, J.L., 2006. Lipids and lipid metabolism in eukaryotic algae.

- 595 Prog. Lipid Res. 45, 160–186. <https://doi.org/10.1016/j.plipres.2006.01.001>
- 596 Hao, X., Luo, L., Jouhet, J., Rébeillé, F., Maréchal, E., Hu, H., Pan, Y., Tan, X., Chen,
597 Z., You, L., Chen, H., Wei, F., Gong, Y., 2018. Enhanced triacylglycerol
598 production in the diatom *Phaeodactylum tricornutum* by inactivation of a Hotdog-
599 fold thioesterase gene using TALEN-based targeted mutagenesis 06 Biological
600 Sciences 0601 Biochemistry and Cell Biology. Biotechnol. Biofuels 11, 1–18.
601 <https://doi.org/10.1186/s13068-018-1309-3>
- 602 Isobe, A., Iwasaki, S., Uchida, K., Tokai, T., 1957. the upper ocean from 1957 to 2066.
603 Nat. Commun. 2030, 1–3. <https://doi.org/10.1038/s41467-019-08316-9>
- 604 Jónasdóttir, S.H., 2019. Fatty Acid Profiles and Production in Marine Phytoplankton.
605 Mar. Drugs 17, 1–20. <https://doi.org/10.3390/md17030151>
- 606 Klein, B., 1988. Variation of pigment content in two benthic diatoms during growth in
607 bath cultures. J. Exp. Mar. Bio. Ecol. 115, 237–248.
- 608 Klimov, V. V, 2014. Discovery of pheophytin function in the photosynthetic energy
609 conversion as the primary electron acceptor of Photosystem II Discovery of
610 pheophytin function in the photosynthetic energy conversion as the primary
611 electron acceptor of Photosystem II. <https://doi.org/10.1023/A>
- 612 Kobayashi, K., 2018. Role of membrane glycerolipids in photosynthesis , thylakoid
613 biogenesis and chloroplast development. J. Plant Res. 129, 565–580.
614 <https://doi.org/10.1007/s10265-016-0827-y>
- 615 Kuczynska, P., Jemiola-Rzeminska, M., Strzalka, K., 2015. Photosynthetic pigments in
616 diatoms. Mar. Drugs 13, 5847–5881. <https://doi.org/10.3390/md13095847>
- 617 Lagarde, F., Olivier, O., Zanella, M., Daniel, P., Hiard, S., Caruso, A., 2016.

- 618 Microplastic interactions with freshwater microalgae: Hetero-aggregation and
619 changes in plastic density appear strongly dependent on polymer type. Environ.
620 Pollut. 215, 331–339. <https://doi.org/10.1016/j.envpol.2016.05.006>
- 621 Lavaud, J., 2007. Fast Regulation of Photosynthesis in Diatoms: Mechanisms ,
622 Evolution and Ecophysiology. Plant Sci. Biotechnol. 1, 267–287.
- 623 Le Grand, F., Soudant, P., Marty, Y., Le Goïc, N., Kraffe, E., 2013. Altered membrane
624 lipid composition and functional parameters of circulating cells in cockles
625 (*Cerastoderma edule*) affected by disseminated neoplasia. Chem. Phys. Lipids
626 167–168, 9–20. <https://doi.org/10.1016/J.CHEMPHYSLIP.2013.01.004>
- 627 Lelong, A., Haberkorn, H., Le Goïc, N., Hégaret, H., Soudant, P., 2011. A New Insight
628 into Allelopathic Effects of *Alexandrium minutum* on Photosynthesis and
629 Respiration of the Diatom *Chaetoceros neogracile* Revealed by Photosynthetic-
630 performance Analysis and Flow Cytometry. Microb. Ecol. 62, 919–930.
631 <https://doi.org/10.1007/s00248-011-9889-5>
- 632 Lenz, R., Enders, K., Stedmon, C.A., MacKenzie, D.M.A., Nielsen, T.G., 2015. A
633 critical assessment of visual identification of marine microplastic using Raman
634 spectroscopy for analysis improvement. Mar. Pollut. Bull. 100, 82–91.
635 <https://doi.org/10.1016/j.marpolbul.2015.09.026>
- 636 Levitan, O., Dinamarca, J., Hochman, G., Falkowski, P.G., 2014. Diatoms: A fossil fuel
637 of the future. Trends Biotechnol. 32, 117–124.
638 <https://doi.org/10.1016/j.tibtech.2014.01.004>
- 639 Li, S., Xu, J., Chen, Jiao, Chen, Juanjuan, Zhou, C., Yan, X., 2014. The major lipid
640 changes of some important diet microalgae during the entire growth phase.
641 Aquaculture 428–429, 104–110. <https://doi.org/10.1016/j.aquaculture.2014.02.032>

- 642 Liang, Y., Maeda, Y., Sunaga, Y., Muto, M., Matsumoto, M., Yoshino, T., Tanaka, T.,
643 2013. Biosynthesis of polyunsaturated fatty acids in the oleaginous marine diatom
644 *Fistulifera* sp. strain JPCC DA0580. *Mar. Drugs* 11, 5008–5023.
645 <https://doi.org/10.3390/md11125008>
- 646 Long, M., Moriceau, B., Gallinari, M., Lambert, C., Huvet, A., Raffray, J., Soudant, P.,
647 2015. Interactions between microplastics and phytoplankton aggregates: Impact on
648 their respective fates. *Mar. Chem.* 175, 39–46.
649 <https://doi.org/10.1016/j.marchem.2015.04.003>
- 650 Long, M., Paul-Pont, I., Hégaret, H., Moriceau, B., Lambert, C., Huvet, A., Soudant, P.,
651 2017. Interactions between polystyrene microplastics and marine phytoplankton
652 lead to species-specific hetero-aggregation. *Environ. Pollut.* 228, 454–463.
653 <https://doi.org/10.1016/j.envpol.2017.05.047>
- 654 Long, M., Tallec, K., Soudant, P., Lambert, C., Le Grand, F., Sarthou, G., Jolley, D.,
655 Hégaret, H., 2018. A rapid quantitative fluorescence-based bioassay to study
656 allelochemical interactions from *Alexandrium minutum*. *Environ. Pollut.* 242,
657 1598–1605. <https://doi.org/10.1016/j.envpol.2018.07.119>
- 658 Manfra, L., Rotini, A., Bergami, E., Grassi, G., Faleri, C., Corsi, I., 2017. Comparative
659 ecotoxicity of polystyrene nanoparticles in natural seawater and reconstituted
660 seawater using the rotifer *Brachionus plicatilis*. *Ecotoxicol. Environ. Saf.* 145,
661 557–563. <https://doi.org/10.1016/j.ecoenv.2017.07.068>
- 662 Mao, Y., Ai, H., Chen, Y., Zhang, Z., Zeng, P., Kang, L., Li, W., Gu, W., He, Q., Li, H.,
663 2018. Phytoplankton response to polystyrene microplastics: Perspective from an
664 entire growth period. *Chemosphere* 208, 59–68.
665 <https://doi.org/10.1016/j.chemosphere.2018.05.170>

- 666 Mari, X., Passow, U., Migon, C., Burd, A.B., Legendre, L., 2017. Transparent
667 exopolymer particles: Effects on carbon cycling in the ocean. *Prog. Oceanogr.* 151,
668 13–37. <https://doi.org/10.1016/j.pocean.2016.11.002>
- 669 Moutel, B., Gonçalves, O., Le Grand, F., Long, M., Soudant, P., Legrand, J., Grizeau,
670 D., Pruvost, J., 2016. Development of a screening procedure for the
671 characterization of *Botryococcus braunii* strains for biofuel application. *Process*
672 *Biochem.* 51, 1855–1865. <https://doi.org/10.1016/J.PROCBIO.2016.05.002>
- 673 Nolte, T.M., Hartmann, N.B., Kleijn, J.M., Garnæs, J., van de Meent, D., Jan Hendriks,
674 A., Baun, A., 2017. The toxicity of plastic nanoparticles to green algae as
675 influenced by surface modification, medium hardness and cellular adsorption.
676 *Aquat. Toxicol.* 183, 11–20. <https://doi.org/10.1016/j.aquatox.2016.12.005>
- 677 Pavlic, Z., Vidakovic´-Cifrek, E., Puntaric, A. 2005. Toxicity of surfactants to green
678 microalgae *Pseudokirchneriella subcapitata* and *Scenedesmus subspicatus* and to
679 marine diatoms *Phaeodactylum tricornutum* and *Skeletonema costatum*.
680 *Chemosphere.* 61, 1061–1068. <https://doi.org/10.1016/j.chemosphere.2005.03.051>
- 681 Pinsino, A., Bergami, E., Torre, C.D., Vannuccini, M.L., Addis, P., Secci, M., Dawson,
682 K.A., Matranga, V., Corsi, I., 2017. Amino-modified polystyrene nanoparticles
683 affect signalling pathways of the sea urchin (*Paracentrotus lividus*) embryos.
684 *Nanotoxicology* 11, 201–209. <https://doi.org/10.1080/17435390.2017.1279360>
- 685 Plastics Europe, EPRO, 2016. Plastics – the Facts 2016. *Plast. – Facts 2016 zu finden*
686 *unter.* [www.plasticseurope.de/informations.](http://www.plasticseurope.de/informations)
687 <https://doi.org/10.1016/j.marpolbul.2013.01.015>
- 688 Pratiwi, A.R., Syah, D., Hardjito, L., Panggabean, L.M.G., Suhartono, M.T., 2009. Fatty
689 Acid Synthesis by Indonesian Marine Diatom, *Chaetoceros gracilis*. HAYATI J.

- 690 Biosci. 16, 151–156. <https://doi.org/10.4308/hjb.16.4.151>
- 691 Prihoda, J., Tanaka, A., De Paula, W.B.M., Allen, J.F., Tirichine, L., Bowler, C., 2012.
692 Chloroplast-mitochondria cross-talk in diatoms. *J. Exp. Bot.* 63, 1543–1557.
693 <https://doi.org/10.1093/jxb/err441>
- 694 Ras, J., Claustre, H., Uitz, J., 2008. Spatial variability of phytoplankton pigment
695 distributions in the Subtropical South Pacific Ocean: Comparison between in situ
696 and predicted data. *Biogeosciences* 5, 353–369. [https://doi.org/10.5194/bg-5-353-](https://doi.org/10.5194/bg-5-353-2008)
697 2008
- 698 Sjollema, S.B., Redondo-Hasselerharm, P., Leslie, H.A., Kraak, M.H.S., Vethaak, A.D.,
699 2016. Do plastic particles affect microalgal photosynthesis and growth? *Aquat.*
700 *Toxicol.* 170, 259–261. <https://doi.org/10.1016/j.aquatox.2015.12.002>
- 701 Summers, S., Henry, T., Gutierrez, T., 2018. Agglomeration of nano- and microplastic
702 particles in seawater by autochthonous and de novo-produced sources of
703 exopolymeric substances. *Mar. Pollut. Bull.* 130, 258–267
- 704 Suroy, M., Moriceau, B., Boutorh, J., Goutx, M., 2014a. Fatty acids associated with the
705 frustules of diatoms and their fate during degradation-A case study in
706 *Thalassiosira weissflogii*. *Deep. Res. Part I Oceanogr. Res. Pap.* 86, 21–31.
707 <https://doi.org/10.1016/j.dsr.2014.01.001>
- 708 Tallec, K., Huvet, A., Di Poi, C., González-Fernández, C., Lambert, C., Petton, B., Le
709 Goïc, N., Berchel, M., Soudant, P., Paul-Pont, I., 2018. Nanoplastics impaired
710 oyster free living stages, gametes and embryos. *Environ. Pollut.* 242, 1226–1235.
- 711 Tallec, K., Blard, O., González-Fernández, C., Brotons, G., Berchel, M., Soudant, P.,
712 Huvet, A., Paul-Pont, I., 2019. Surface functionalization determines behavior of

- 713 nanoplastic solutions in model aquatic environments. *Chemosphere* 225, 639–646.
714 <https://doi.org/10.1016/j.chemosphere.2019.03.077>
- 715 Tanaka, A., De Martino, A., Amato, A., Montsant, A., Mathieu, B., Rostaing, P.,
716 Tirichine, L., Bowler, C., 2015. Ultrastructure and Membrane Traffic During Cell
717 Division in the Marine Pennate Diatom *Phaeodactylum tricornutum*. *Protist* 166,
718 506–521. <https://doi.org/10.1016/j.protis.2015.07.005>
- 719 Ter Halle, A., Jeanneau, L., Martignac, M., Jardé, E., Pedrono, B., Brach, L. 2017.
720 Nanoplastic in the north atlantic subtropical gyre. *Envir. Sci. Technol.* 51, 13689–
721 13697. doi: 10.1021/acs.est.7b03667
- 722 Thompson, G.A., 1996. Review: Lipids and membran function in green algae. *Biochim.*
723 *Biophys. Acta.* 1302, 17–45.
- 724 Walsh, P.J., Clarke, S.A., Julius, M., Messersmith, P.B., 2017. Exploratory Testing of
725 Diatom Silica to Map the Role of Material Attributes on Cell Fate. *Sci. Rep.* 7, 1–
726 13. <https://doi.org/10.1038/s41598-017-13285-4>
- 727 Yi, Z., Xu, M., Di, X., Brynjolfsson, S., Fu, W., 2017. Exploring Valuable Lipids in
728 Diatoms. *Front. Mar. Sci.* 4, 1–10. <https://doi.org/10.3389/fmars.2017.00017>
- 729 Zhang, C., Chen, X., Wang, J., Tan, L., 2017. Toxic effects of microplastic on marine
730 microalgae *Skeletonema costatum*: Interactions between microplastic and algae.
731 *Environ. Pollut.* 220, 1282–1288. <https://doi.org/10.1016/j.envpol.2016.11.005>
- 732 Zigmantas, D., Hiller, R.G., Sharples, F.P., Frank, H.A., Sundström, V., Polívka, T.,
733 2004. Effect of a conjugated carbonyl group on the photophysical properties of
734 carotenoids. *Phys. Chem. Chem. Phys.* 6, 3009–3016.
735 <https://doi.org/10.1039/b315786e>

- 736 Zulu, N.N., Zienkiewicz, K., Vollheyde, K., Feussner, I., 2018. Progress in Lipid
737 Research. Prog. Lipid Res. 70, 1–16. <https://doi.org/10.1016/j.plipres.2018.03.001>

Journal Pre-proof

Figure captions

Figure 1. Main lipid classes of *C. neogracile* after exposure to two concentrations of nanoplastics for 96 hours, expressed as $\mu\text{g lipid } 10^{-6} \text{ cells}$ (mean \pm standard deviation, $n=3$). A: exponential growth phase and B: stationary growth phase. Letters indicate significant differences between treatments (*I-Way-ANOVA* analysis) with significant values as $p<0.05$. PC: phosphatidyl choline, PE+PG+SQDG: sum of phosphatidyl ethanolamine, phosphatidyl glycerol and sulfoquinovosyl-diacylglycerol, PI: phosphatidylinositol, PS: phosphatidylserine, MGDG: monogalactosyl-diacylglycerol, DGDG: digalactosyl-diacylglycerol, FST: free sterols, FFA: free fatty acids and TAG: triglycerides.

Figure 2. Ratio of monogalactosyl-diacylglycerol and digalactosyl-diacylglycerol (MGDG/DGDG) of *C. neogracile* after exposure to two concentrations (0.05 and $5 \mu\text{g mL}^{-1}$) of nanoplastics for 96 hours (mean \pm standard deviation, $n=3$). Letters indicate significant differences between treatments (*I-Way-ANOVA* analysis) with significant values as $p<0.05$

Figure 3. Neutral lipid content of *C. neogracile* after 96 hours exposure to 0.05 and $5 \mu\text{g mL}^{-1}$ PS-NH₂ expressed as arbitrary units (mean \pm standard deviation, $n=3$). Letters indicate significant differences between treatments (*I-Way-ANOVA* analysis) with significant values as $p<0.05$

Figure 4. Principal component analysis of *C. neogracile*' fatty acid composition exponential cultures exposed to two concentrations of PS-NH₂ for 96 hours. A, B: polar lipid fraction and C,D: neutral lipid fraction

Table 1. Pigment composition of *C. neogracile* after exposure to two concentrations of PS-NH₂ for 4 days. Pigments are expressed as mean ± standard deviation (n=3) of peak area (sample corresponding to 2×10^7 cells in each condition). Letters show differences between treatments within the same growth stage. Significant levels are considered as $p < 0.05$. Chl *a*: chlorophyll *a*, Allo Chl *a*: allo chlorophyll *a*, Epi Chl *a*: epi chlorophyll *a*, Chl *c2*: chlorophyll *c2*, Fx: fucoxanthin, Nx: neoxanthin Vx: violaxanthin, Ddx: diadinoxanthin, Dtx: diatoxanthin, Phx: phaeophytin and β-car: β-carotene.

Pigment	<i>Exponential stage</i>			<i>Stationary stage</i>		
	Control	Low	High	Control	Low	High
Chl <i>a</i>	4205±301 b	3641±726 b	990±273 a	224±73	167±16	150±17
Allo Chl <i>a</i>	995±66 c	708±81 b	33±0.9 a	14±5	10±0.3	10±0.2
Epi Chl <i>a</i>	66±3 b	53±10 b	14±4 a	4±1	2±0.3	2±0.3
Chl <i>c2</i>	695±81 b	579±194 b	143±63 a	21±11 b	17±0.9 a	15±0.6 a
Fx	3079±70 b	2461±567 b	518±192 a	132±48	103±6	103±17
Nx	11±1	11±2	8±1	1±0.4	0.9±0.1	0.8±0.1
Vx	7±0.3	5±1	6±0.9	0.6±0.2	0.5±0.1	0.5±0.1
Ddx	834±98 b	848±169 b	269±59 a	42±14	35±1	37±6
Dtx	6±0.6 a	7±1 a	26±4 b	15±5	11±1	11±1
Phx	354±42 b	278±5 b	87±35 a	19±5 b	3±2 a	0.0 a
β-car	85±18 b	70±10 b	31±11 a	3±1 b	1±0.2 a	0.8±0.1 a

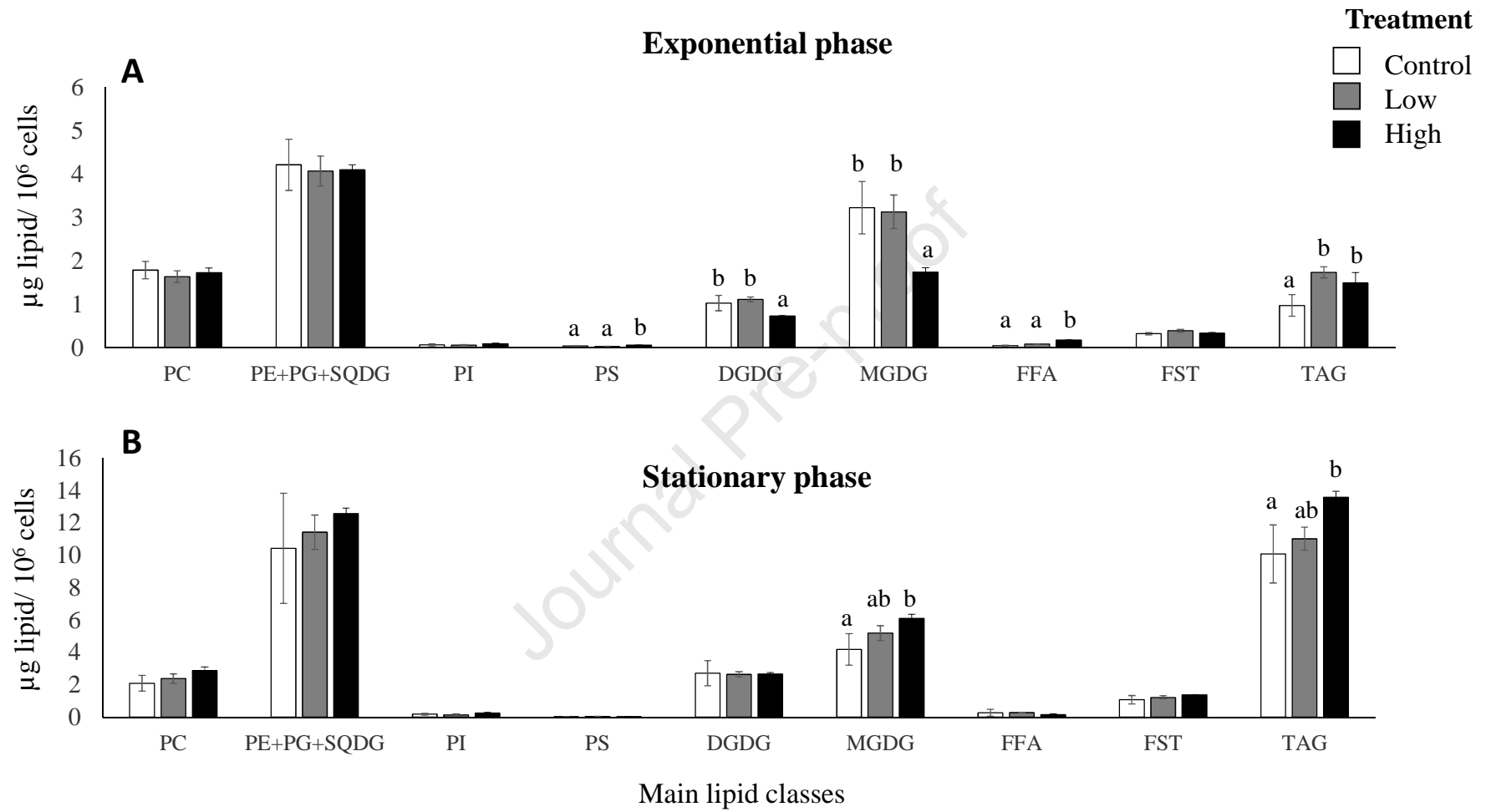


Figure 1

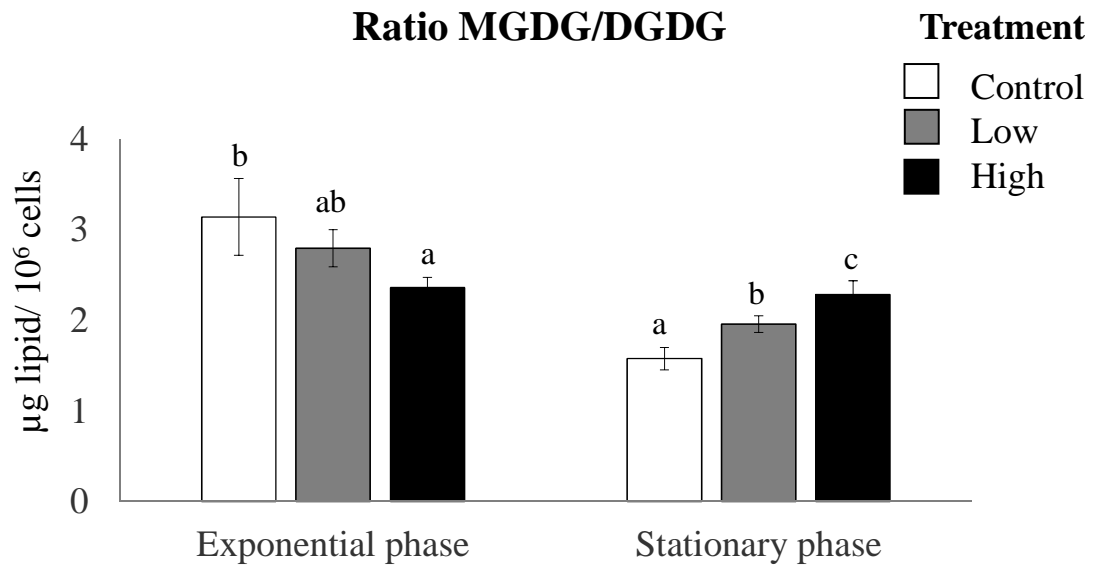


Figure 2

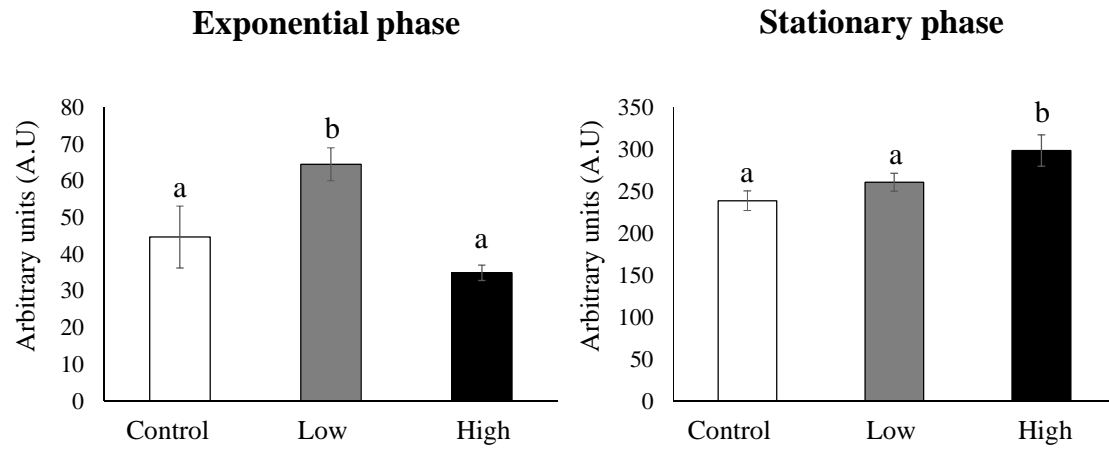
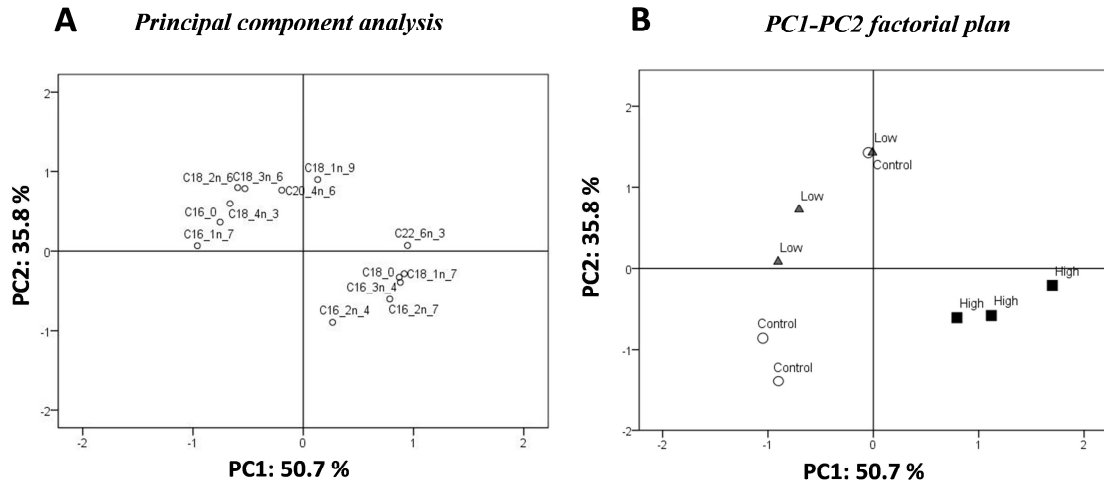


Figure 3

Polar lipid fraction



Neutral lipid fraction

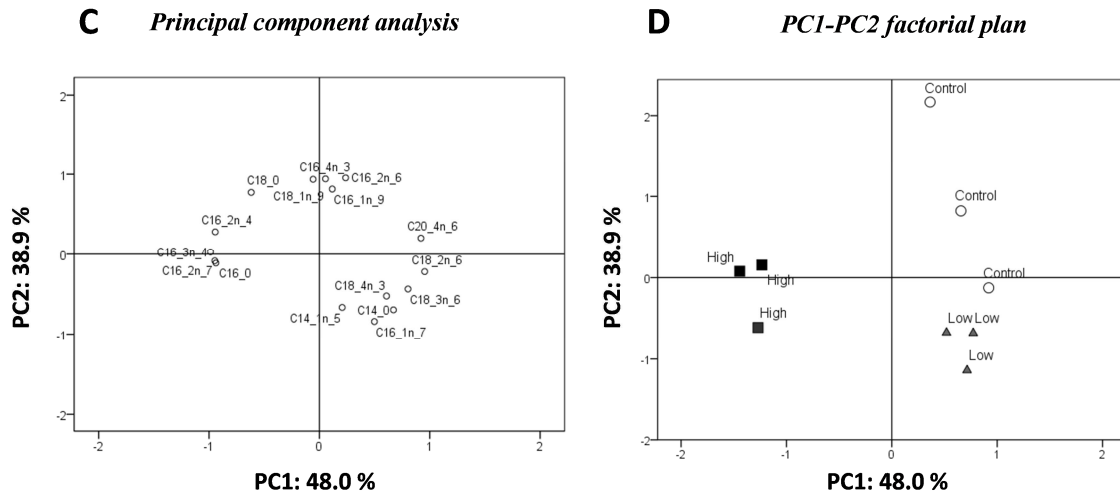


Figure 4

Highlights:

1. Nanoplastics (NP) effect on algae was studied at exponential and stationary phase
2. NP impact pigment and lipid composition of diatoms at both growth phases
3. Algae adjust their thylakoid membrane lipid composition to cope with NP stress
4. Algae physiological state is a determinant factor to evaluate NP impact on diatoms

Journal Pre-proof

All the authors participated in the elaboration of this research article.

C. González Fernández performed the experimental design, did the experiment and write the original draft. She also participated on the revision process.

A. Bideau performed lipid analysis. F. Le Grand supervised and validated lipid analysis.

A. Huvet and I. Paul-Pont participated in the elaboration of the manuscript and the process of revision.

P. Soudant participate in the validation of the results, elaboration of the manuscript, review process and funding acquisition.

Journal Pre-proof

Declaration of interests

The authors declare that they have no known competing financial interests or personal relationships that could have appeared to influence the work reported in this paper.

The authors declare the following financial interests/personal relationships which may be considered as potential competing interests: